Published by
NIGERIAN SOCIETY OF PHYSICAL SCIENCES
Available online @ https://journal.nsps.org.ng/index.php/jnsps

J. Nig. Soc. Phys. Sci. 3 (2021) 38–41

Journal of the Nigerian Society of Physical Sciences

# Velocity distribution of $^{43}Ca^{+}$ ion cloud in the low temperature limit in a quadrupole Penning Trap

Dyavappa B. M.*

*Department of Physics, Government First Grade College for Women, Kolar, India*

## Abstract

Penning trap has electric field created by DC voltage applied between ring and end cap electrodes and magnetic field is applied along symmetry axis, as the electric field confines ions in the axial direction through an electric potential minimum and the magnetic field confines the ions in the radial direction. The trapping potential created by the DC voltage applied between the end cap and ring electrodes in the low temperature limit is cancelled by Coulomb interaction of ions and the total energy is mainly kinetic energy of ions. The velocity distribution of $^{43}Ca^{+}$ ions along axial direction, in radial plane and total velocity distribution due to resulting motion of both axial and radial motion of ions in low temperature limit in a Quadrupole Penning trap are presented here. These results reveal the properties of $^{43}Ca^{+}$ ion cloud and are useful to study confining techniques for different types of ions in low temperature limit and a qubit can be encoded in the hyperfine ground states of $^{43}Ca^{+}$ isotope for ion trap quantum computation.

DOI:10.46481/jnsps.2021.132

*Keywords:* Quadrupole Penning trap, Velocity distribution function, $^{43}Ca^{+}$ cloud.

*Article History :*
Received: 08 August 2020
Received in revised form: 24 January 2021
Accepted for publication: 29 January 2021
Published: 27 February 2021

©2021 Journal of the Nigerian Society of Physical Sciences. All rights reserved.
Communicated by: B. J. Falaye

## 1. Introduction

$^{43}Ca^{+}$ ion has only one valence electron and has simple energy level structure, has long-lived D-states, therefore it can be used for quantum computation [1, 2, 3], for building an ion clock [4] and also for laser cooling. The large fine-structure splitting of $\Delta\nu_{FS} = 6.7THz$ between the $P_{1/2}$ and $P_{3/2}$ states in $^{43}Ca^{+}$ion as shown in Figure 1 allows a large detuning of the Raman light fields from the $P-$ levels and thus high fidelity gate operations, as spontaneous emission processes are largely suppressed, which is requirement for ion trap quantum computation. And encoding the qubit in the hyperfine ground states ensures that decay from spontaneous emission is completely avoided and thus, very long coherence times may be achieved potentially and the qubits will ideally depend only in second order on the external magnetic field [5]. A thorough knowledge of different properties of ions including velocity distribution along axial direction, in radial plane and the total velocity distribution is necessary. The quadrupole Penning trap is made with two end-cap electrodes and a ring electrode. The equation of ring electrode is $\frac{r^2}{r_0^2} - \frac{z^2}{z_0^2} = +1$ and equations of two similar end-cap electrodes is $\frac{r^2}{r_0^2} - \frac{z^2}{z_0^2} = -1$, where $r_0$ is the inner radius of the ring electrode in the radial plane and $z_0$ is half of the vertical distance between the two end-cap electrodes such that $r_0 = \sqrt{2}\, z_0$. The trap potential created by the DC voltage applied between

*Corresponding author tel. no: +91 9483113600
*Email address:* dyavappabm@gmail.com (Dyavappa B. M. )

the end cap and ring electrodes is given by [6, 7].

$$V(r,z) = \frac{V_0}{r_0^2 + 2z_0^2}\left(2z^2 - r^2\right) \tag{1}$$

The vector potential of the magnetic field $\boldsymbol{B}$ is [4, 5]

$$\boldsymbol{A} = \frac{1}{2}(\boldsymbol{B} \times \boldsymbol{r}) = \frac{1}{2}B(-y\hat{\boldsymbol{x}} + x\hat{\boldsymbol{y}}) \tag{2}$$

The Lorenz force in an electromagnetic field with an electric field $\boldsymbol{E}$ and magnetic field $\boldsymbol{B}$ on $^{43}Ca^{+}$ion of mass $m$, charge $q$, moving with a velocity $\boldsymbol{v}$ is given by [8]

$$\boldsymbol{F} = q\left[\boldsymbol{E} + (\boldsymbol{v} \times \boldsymbol{B})\right] \tag{3}$$

$$\boldsymbol{F} = q\left[\left(\frac{2V_0}{d^2}x\hat{\boldsymbol{x}} + \frac{2V_0}{d^2}y\hat{\boldsymbol{y}} - \frac{4V_0}{d^2}z\hat{\boldsymbol{z}}\right) + B\left(\dot{y}\hat{\boldsymbol{x}} - \dot{x}\hat{\boldsymbol{y}}\right)\right] \tag{4}$$

The axial, pure cyclotron, reduced cyclotron and magnetron frequencies of $^{43}Ca^{+}$ion are given respectively by [9, 10, 11]

$$f_z = \frac{1}{2\pi}\sqrt{\frac{4qV_0}{md^2}}, \quad f_c = \frac{qB}{2\pi m}$$
$$f_c' = \frac{f_c + \sqrt{f_c^2 - 2f_z^2}}{2}, \quad f_m = \frac{f_c - \sqrt{f_c^2 - 2f_z^2}}{2} \tag{5}$$

The velocities of $^{43}Ca^{+}$ion in the axial direction, radial plane and in space are

$$v_z = \sqrt{\frac{k_BT}{m}}, \quad v_r = \sqrt{\frac{2k_BT}{m}}, \quad v = \sqrt{\frac{3k_BT}{m}} \tag{6}$$

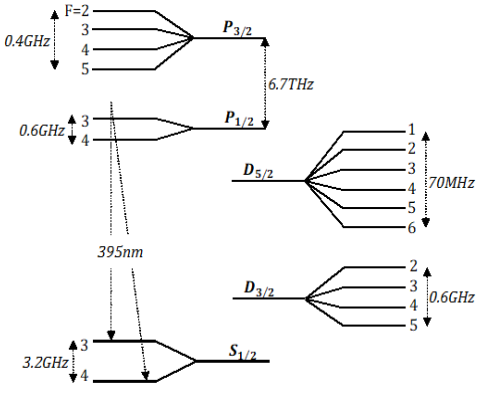


Figure 1: Energy level scheme of $^{43}Ca^{+}$ isotope, a qubit can be encoded in the hyperfine ground states for ion trap quantum computation [5]

## 2. Theory

We assume that the $^{43}Ca^{+}$ion cloud is in thermal equilibrium through electrostatic Coulomb interaction between ions. The rotation of $^{43}Ca^{+}$ion cloud in magnetic field is equivalent to neutralization by opposite charge of ions and the distribution of magnetically confined ions in thermal equilibrium without rotation can be treated as ions confined and neutralized by a

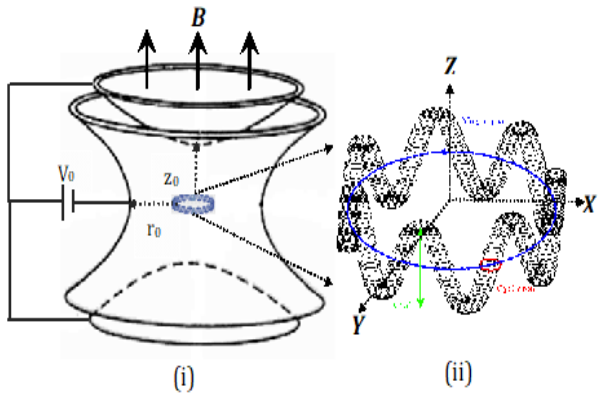


Figure 2: (i)**:** Penning trap with $^{43}Ca^{+}$ions confined in trap space, $\boldsymbol{B}$: Magnetic Field, $V_0$: storage voltage, (ii) Magnified view of motion of a $^{43}Ca^{+}$ions confined in trap space in a Penning trap showing reduced cyclotron, magnetron and axial motions

cylinder of opposite charge. The probability of velocity distribution in thermal-equilibrium is [12]

$$d\mathcal{P}\left(v_{r,\phi,z}\right) = \frac{2\pi}{(\pi kT)^{3/2}}\left(\frac{m}{2}\right)^{1/2} v \times \exp\left[-m\left(\frac{v^2 - \omega_\phi v_\phi/2)}{2k_BT}\right)\right] drd\phi dz dv_r dv_\phi dv_z \tag{7}$$

where $\omega_\phi$ is the rotational frequency of $^{43}Ca^{+}$ion cloud as a whole determined by the temperature of the ion cloud. The Energy of single $^{43}Ca^{+}$ion is [12]

$$E = \frac{m}{2}\left[v_r^2 + \left(\frac{v_\phi}{r} - \frac{qBr}{2mc}\right)^2 + v_z^2\right] + q\left[V_T(r,z) + V_q(r,z)\right] \tag{8}$$

The momenta in radial plane, azimuthal and axial directions are [12]

$$P_r = mv_r = m\frac{dr}{dt}, \quad P_\phi = mr^2\frac{d\phi}{dt} + \frac{qB}{2c}r^2 = mrv_\phi - \frac{\omega_c}{2}mr^2,$$
$$P_z = m\frac{dz}{dt} = mv_z \tag{9}$$

### 2.1. Velocity distribution of $^{43}Ca^{+}$ ion cloud at the low temperature limit

In a Penning trap $^{43}Ca^{+}$ ions are confined in the low temperature limit when the electrostatic potential energy [12]

$$qV_q(r,z) \gg k_BT \tag{10}$$

$$qV_T(r,z) + qV_q(r,z) + \frac{m}{2}\omega_\phi\left(\omega_c - \omega_\phi\right)r^2 = 0 \tag{11}$$

The energy along the axial direction in the low temperature limit is [12]

$$E_z = \frac{1}{2}mv_z^2 = \frac{1}{2}k_BT \tag{12}$$

The energy in the radial plane in the low temperature limit is [12]

$$E_r = \frac{1}{2}\left(mv_r^2 + \frac{mv_\phi^2}{r^2}\right) + \left(\frac{\omega_c^2}{8}\right)r^2 + \frac{\omega_c}{2}v_\phi \tag{13}$$

If we neglect Coulomb interaction potential $V_q(r,z)$ then the probability of velocity distribution in the low temperature limit is [12]

$$d\mathcal{P}\left(E_{v_r,v_\phi,v_z}\right) = A'''exp\left[-m\left(\frac{v_z^2+v_r^2}{2k_BT}\right)\right]dv_r d\left(\frac{v_\phi}{r}\right)dv_z \quad (14)$$

The probability of velocity distribution in Z-direction in the low temperature limit is [12]

$$d\mathcal{P}(v_z) = \left(\frac{2}{\pi m k_B T}\right)^{1/2} exp\left[-\left(\frac{mv_z^2}{2k_BT}\right)\right]v_z dv_z \quad (15)$$

The probability density of velocity distribution in Z-direction in the low temperature limit is [12]

$$\rho_z(v_z) = \left(\frac{2}{\pi m k_B T}\right)^{1/2}\left[exp\left(-\frac{1}{2}\frac{mv_z^2}{k_BT}\right)\right]v_z \quad (16)$$

The probability density of velocity distribution in axial direction increases sharply up to $\sqrt{mv_z^2/2k_BT} = 0.854$ at $\rho_z = 3.019\times 10^{25}$, decreases abruptly and remains almost a constant in low temperature limit as shown in Figure 3.

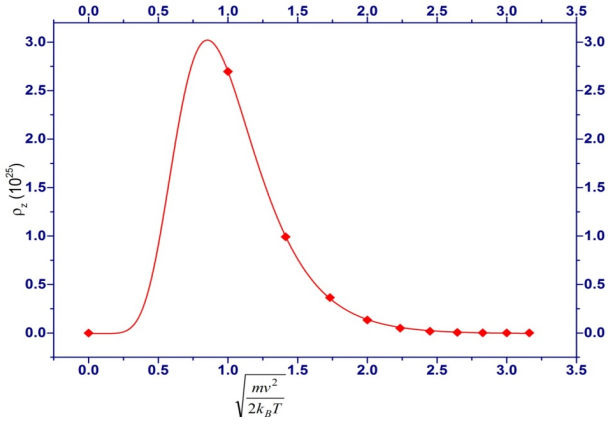


Figure 3: The axial probability density of velocity of $^{43}Ca^{+}$ion cloud in the low temperature limit

The probability of velocity distribution in the radial plane in the low temperature limit is [12]

$$d\mathcal{P}\left(v_{r,\phi}\right) = \left(\frac{1}{k_BT}\right)exp\left(-\frac{1}{2}\frac{mv_r^2}{k_BT}\right)mv_r dv_r \quad (17)$$

The probability density of velocity distribution in radial plane in the low temperature limit is [12]

$$\rho_r(v_r) = \left(\frac{1}{k_BT}\right)exp\left(-\frac{1}{2}\frac{mv_r^2}{k_BT}\right) \quad (18)$$

The probability density of velocity distribution in radial plane increases sharply up to $\sqrt{mv_r^2/2k_BT} = 1.4072$ at $\rho_r = 4.89\times 10^{22}$, decreases abruptly and remains almost a constant in low temperature limit as shown in Figure 4

The total probability of velocity distribution is [12]

$$d\mathcal{P}(v) = \left(\frac{2m}{\pi}\right)^{\frac{1}{2}}\left(\frac{1}{k_BT}\right)^{\frac{3}{2}}exp\left(-\frac{1}{2}\frac{mv^2}{k_BT}\right)vdv \quad (19)$$

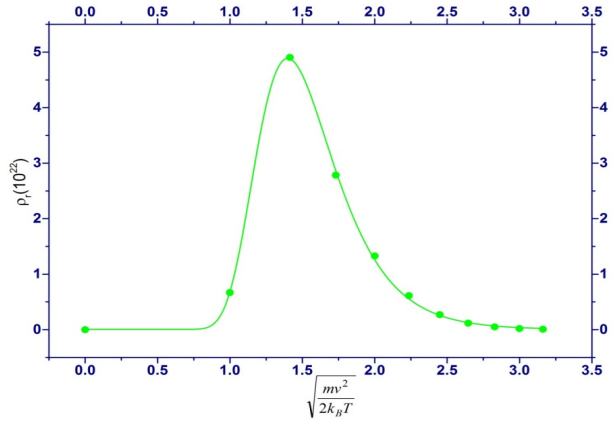


Figure 4: The radial probability density of velocity of $^{43}Ca^{+}$ion cloud in the low temperature limit

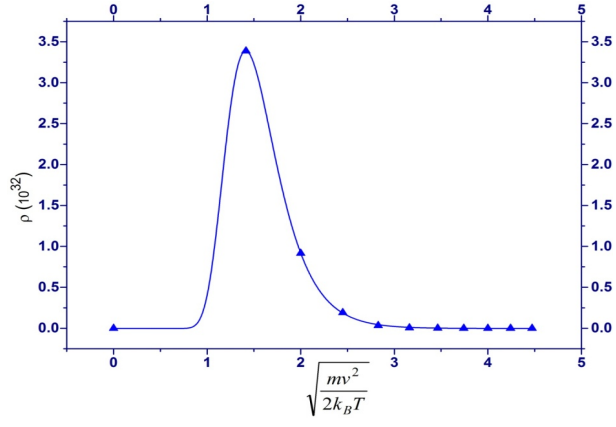


Figure 5: The total probability density of velocity of $^{43}Ca^{+}$ion cloud in the low temperature limit

The total probability density of velocity distribution is [12]

$$\rho(v) = \left(\frac{2m}{\pi}\right)^{\frac{1}{2}}\left(\frac{1}{k_BT}\right)^{\frac{3}{2}}exp\left(-\frac{1}{2}\frac{mv^2}{k_BT}\right)v \quad (20)$$

The total probability density of velocity distribution in trapping region increases sharply up to $\sqrt{mv^2/2k_BT} = 1.4086$ at $\rho = 3.399\times 10^{32}$, decreases abruptly and remains almost a constant in low temperature limit as shown in Figure 5. The axial, radial and total probability densities of velocity distribution increase sharply up to $\sqrt{mv_z^2/2k_BT} = 0.854$, $\sqrt{mv_r^2/2k_BT} = 1.4072$ and $\sqrt{mv^2/2k_BT} = 1.4086$ respectively, at $\rho_z = 3.019\times 10^{25}$, $\rho_r = 4.89\times 10^{22}$and $\rho = 3.399\times 10^{32}$ respectively, beyond which decrease abruptly, remain almost constant for the low temperature limit as shown in the Figure 6. The radial probability density of velocity distribution is less than the axial probability density of velocity distribution, which in turn less than the total probability density of velocity distribution.

## 3. Conclusion

The probability density of velocity distribution of $^{43}Ca^{+}$ion cloud along axial direction and in radial plane together results

Table 1: The values of axial, radial and total probability densities of velocity of $^{43}Ca^{+}$ion cloud in the low temperature limit

| $\frac{mv^2}{2k_BT}$ | $\sqrt{\frac{mv^2}{2k_BT}}$ | $T\ (K)$ | $k_BT\left(10^{-23}J\right)$ | $\rho_z\left(v_z\right)\left(10^{25}\right)$ | $\rho_r\left(v_r\right)\left(10^{22}\right)$ | $\rho\left(v\right)\left(10^{32}\right)$ |
|---|---|---|---|---|---|---|
| 0 | 0 | $\infty$ | $\infty$ | 0 | 0 | 0 |
| 2 | 1.4142 | 4 | 5.52 | 2.69719 | 0.66645 | 3.3882 |
| 4 | 2 | 2 | 2.76 | 0.992243 | 4.9034 | 0.9171 |
| 6 | 2.4495 | 1.3 | 1.79 | 0.365019 | 2.7814 | 0.19158 |
| 8 | 2.8284 | 1 | 1.38 | 0.134288 | 1.3272 | 0.03359 |
| 10 | 3.1623 | 0.8 | 1.1 | 0.04940 | 0.61254 | 0.005714 |
| 12 | 3.4641 | 0.6667 | 0.92 | 0.018174 | 0.26943 | 0.0009229 |
| 14 | 3.7417 | 0.57 | 0.7866 | 0.006686 | 0.11593 | 0.000149 |
| 16 | 4 | 0.5 | 0.69 | 0.0024595 | 0.048617 | 0.00002253 |
| 18 | 4.2426 | 0.44 | 0.6 | 0.0009048 | 0.020568 | 0.0000035288 |
| 20 | 4.4721 | 0.4 | 0.55 | 0.00033286 | 0.0082545 | 0.000000657 |

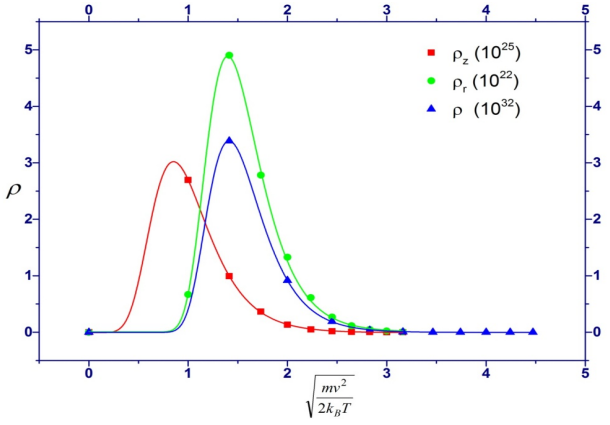


Figure 6: The axial, radial and total probability density of velocity of $^{43}Ca^{+}$ion cloud in the low temperature limit

total probability density of velocity distribution under low temperature limit. The radial probability density of velocity distribution is less than the axial probability density of velocity distribution, which in turn less than the total probability density of velocity distribution. These results reveal the velocity properties of the $^{43}Ca^{+}$ion cloud and are useful to design and carry out experiments on stored $^{43}Ca^{+}$ ions, with velocity related parameters under low temperature limit and also for ion trap quantum computation in Quadrupole Penning trap.

## References


[1] A. Steane, "The ion trap quantum information processor", Applied Physics B: Lasers and Optics **64** (1997) 623.

[2] C. D. Bruzewicz et al., "Dual-species, multi-qubit logic primitives for Ca+/Sr+ trapped-ion Crystals", npj. Quantum Information **5** (2019) 102.

[3] Kylie Foy, "Qubits made from strontium and calcium ions can be precisely controlled by technology that already exists, Massachusetts Institute of Technology", (2020). `https://phys.org/news/2020-01-qubits-strontium-calcium-ions-precisely.html`.

[4] C. Champeneois, M. bHoussin, C. Lisowski, A. Knoop, G. Hagel, A. Vedel & F. Vedel, "Evaluation of the ultimate performances of a $^{43}Ca^{+}$ single-ion frequency standard", Physics Letters A **331** (2004) 298.

[5] R. Blatt, H. Haffner, C. Roos, C. Becher & F. Schmidt-Kaler, "Ion Trap Quantum Computing with $Ca^{+}$ Ions", Quantum Information Processing **3** (2004) 1.

[6] F. G. Major, V. N. Gheorghe & G. Werth, *Charged Particle Traps, Physics and techniques of charged particle confinement*, Springer Publishers (2005).

[7] P. K. Ghosh, *Ion Traps*, Clarendon Press, Oxford, (1995) 72.

[8] B. M. Dyavappa, "Spectroscopy of non-neutral plasmas in ion traps" Ph.D thesis, Bangalore University, (2017).

[9] D. Datar, B. M. Dyavappa, B. L. Mahesh, K. T. Satyajith & S. Ananthamurthy, "Energy distribution of electrons under axial motion in a quadrupole Penning trap". Can. J. Phys **94** (2016) 1245.

[10] B. M. Dyavappa, "Velocity distribution of electrons along the symmetry axis of Quadrupole Penning trap", Discovery **56** (2020) 138.

[11] B. M. Dyavappa, D. D. Prakash & S. Ananthamurthy, "Dependence of the confinement time of an electron plasma on the magnetic field in a quadrupole Penning trap", EPJ Techniques and Instrumentation **4** (2017) 4.

[12] G. Z. Li & G. Werth, "Energy distribution of ions in Penning trap", International Journal of Mass Spectrometry and Ion Processes **121** (1992) 65.